Eur. Phys. J. C (2016) 76:624
DOI 10.1140/epjc/s10052-016-4476-z

THE EUROPEAN PHYSICAL JOURNAL C

Regular Article - Theoretical Physics

Possible pentaquarks with heavy quarks

Hongxia Huang[1,2], **Chengrong Deng**[3], **Jialun Ping**[1,a], **Fan Wang**[4]

[1] Department of Physics and Jiangsu Key Laboratory for Numerical Simulation of Large Scale Complex Systems, Nanjing Normal University, Nanjing 210023, People's Republic of China
[2] Department of Physics, Duke Univeristy, Durham, North Carolina 27708, USA
[3] School of Mathematics and Physics, Chongqing Jiaotong University, Chongqing 400074, People's Republic of China
[4] Department of Physics, Nanjing University, Nanjing 210093, People's Republic of China

Received: 27 August 2016 / Accepted: 31 October 2016 / Published online: 16 November 2016

Abstract Inspired by the discovery of two pentaquarks $P_c(4380)$ and $P_c(4450)$ at the LHCb detector, we study possible hidden-charm molecular pentaquarks in the framework of quark delocalization color screening model. Our results suggest that both $N\eta_c$ with $IJ^P = \frac{1}{2}\frac{1}{2}^-$ and NJ/ψ with $IJ^P = \frac{1}{2}\frac{3}{2}^-$ are bounded by channels coupling. However, NJ/ψ with $IJ^P = \frac{1}{2}\frac{3}{2}^-$ may be a resonance state in the D-wave $N\eta_c$ scattering process. Moreover, $P_c(4380)$ can be explained as the molecular pentaquark of $\Sigma_c^* D$ with quantum numbers $IJ^P = \frac{1}{2}\frac{3}{2}^-$. The state $\Sigma_c^* D^*$ with $IJ^P = \frac{1}{2}\frac{5}{2}^-$ is a resonance, it may not be a good candidate of the observed $P_c(4450)$ because of the opposite parity of the state to $P_c(4380)$, although the mass of the state is not far from the experimental value. In addition, the calculation is extended to the hidden-bottom pentaquarks, and similar properties to that of hidden-charm pentaquarks system are obtained.

1 Introduction

Multi-quark states were studied even before the advent of quantum chromodynamics (QCD). The development of QCD accelerated multi-quark study because it is natural in QCD that there should be multi-quark states, glueballs, and quark–gluon hybrids. After more than 40 years of quark-model study, the ideas of a baryon and a meson is about to go beyond the naive picture: q^3 baryon and $q\bar{q}$ meson. The proton spin puzzle could be explained by introducing the $q^3q\bar{q}$ component in the quark model [1,2]. In order to understand the baryon spectroscopy better, the five-quark component of the proton was proposed [3]. The baryon resonance is certainly coupled to the meson–baryon scattering state and should be studied by coupling q^3 with q^3–$q\bar{q}$ scattering channel in a quark-model approach. Although the strange pentaquark state Θ^+ claimed by experimental groups 13 years ago might be questionable (the LEPS Collaboration insists on the existence of the pentaquark Θ^+ [4]) and the multi-quark states might be hard to identify, the multi-quark study is indispensable for understanding the low energy QCD, because the multi-quark states can provide information unavailable in the $q\bar{q}$ meson and the q^3 baryon, especially the property of a hidden color structure.

In the past decade, many near-threshold charmonium-like states have been observed at Belle, BaBar, BESIII, and LHCb, triggering lots of studies on the molecule-like hadrons containing heavy quarks. In the heavy quark sector, the large masses of the heavy quarks reduce the kinetic of the system, which makes it easier to form bound states or resonances. So the heavy quarks play an important role to stabilize the multi-quark systems. There were many theoretical studies of hidden-charm pentaquarks [5–9], especially the prediction of narrow N^* and Λ^* resonances with hidden charm above 4 GeV by using the coupled-channel unitary approach [5,6], and the systematical investigation of possible hidden-charm molecular baryons with components of an anti-charmed meson and a charmed baryon within the one boson exchange model [7].

Very recently, the LHCb Collaboration observed two pentaquark–charmonium states in the $J/\psi p$ invariant mass spectrum of $\Lambda_b^0 \to J/\psi K^- p$ [10]. One is $P_c(4380)$ with a mass of $4380 \pm 8 \pm 29$ MeV and a width of $205 \pm 18 \pm 86$ MeV, and another is $P_c(4450)$ with a mass of $4449.8 \pm 1.7 \pm 2.5$ MeV and a width of $39 \pm 5 \pm 19$ MeV. The preferred J^P assignments are of opposite parity, with one state having spin $\frac{3}{2}$ and the other $\frac{5}{2}$. A lot of theoretical work has been done to explain these two states. In Ref. [11], the current experimental progress and theoretical interpretations of the states were reviewed. Chen et al. [12] interpreted these two hidden-charm states as the loosely bound $\Sigma_c(2455)D^*$ and

[a] e-mail: jlping@njnu.edu.cn

$\Sigma_c^*(2520)D^*$ molecular states by using the boson exchange model, and gave the spin parity $J^P = \frac{3}{2}^-$ and $\frac{5}{2}^-$, respectively. In Ref. [13], a Bethe–Salpeter equation approach was used to studied the $\bar{D}\Sigma_c^*$ and $\bar{D}^*\Sigma_c$ interactions, and then $P_c(4380)$ and $P_c(4450)$ were identified as $\bar{D}\Sigma_c^*$ and $\bar{D}^*\Sigma_c$ molecular states with the spin parity $J^P = \frac{3}{2}^-$ and $\frac{5}{2}^+$, respectively. A QCD sum rule investigation was performed, by which $P_c(4380)$ was suggested to be a $\bar{D}^*\Sigma_c$ hidden-charm pentaquark with $J^P = \frac{3}{2}^-$ and the $P_c(4450)$ was proposed as a mixed hidden-charm pentaquark of $\bar{D}^*\Lambda_c$ and $\bar{D}^*\Sigma_c$ with $J^P = \frac{5}{2}^+$ [14]. Also a coupled-channel calculation was performed to analyze the $\Lambda_b^0 \to J/\psi K^- p$ reaction and gave support to a $J^P = \frac{3}{2}^-$ assignment to $P_c(4450)$ and to its nature as a molecular state mostly made of $\bar{D}^*\Sigma_c$ and $\bar{D}^*\Sigma_c^*$ [15]. In Ref. [16], Meißner and Oller suggested that $P_c(4450)$ was almost entirely a $\chi_{c1}p$ resonance, coupling much more strongly to this channel than to $J/\psi p$. Kubarovsky and Voloshin [17] showed that the observed P_c resonances are composites of J/ψ and excited nucleon states with the quantum numbers of $N(1440)$ and $N(1520)$ within a simple "baryocharmonium" model. Moreover, some people proposed various rescattering mechanisms to show that the $P_c(4450)$ state might arise from the kinematical effect [18,19]. Besides, Burns [20] explored the phenomenology of the $P_c(4380)$ and $P_c(4450)$ states, and their possible partners. Several intriguing similarities were also discussed in Ref. [20], which suggested that $P_c(4450)$ was related to the $X(3872)$ meson. Thus, different models may give different descriptions for the resonance structures. Clearly the quark level study of these two pentaquark-charmonium states is interesting and necessary.

It is well known that the nuclear force (the interaction between nucleons) is qualitatively similar to the molecular force (the interaction between atoms). This molecular model of nuclear forces, the quark delocalization color screening model (QDCSM) [21,22], has been developed and extensively studied. In this model, quarks confined in one nucleon are allowed to delocalize to a nearby nucleon and the confinement interaction between quarks in different baryon orbits is modified to include a color screening factor. The latter is a model description of the hidden color channel-coupling effect [23]. The delocalization parameter is determined by the dynamics of the interacting quark system, and it thus allows the quark system to choose the most favorable configuration through its own dynamics in a larger Hilbert space. The model gives a good description of nucleon–nucleon and hyperon–nucleon interactions and the properties of the deuteron [24–28]. It is also employed to calculated the baryon–baryon scattering phase shifts and the dibaryon candidates in the framework of the resonating group method (RGM) [29–31].

In this work, the resonating-group method (RGM) is employed to study the possible hidden-charm molecular pentaquarks in QDCSM, and the channel-coupling effect are considered. Extension to the bottom case is straightforward and is also included in the present work. The structure of this paper is as follows. After the introduction, we present a brief introduction of the quark model used in Sect. 2. Section 3 is devoted to the numerical results and discussions. A summary is presented in the last section.

2 The quark delocalization color screening model (QDCSM)

The details of the QDCSM used in the present work can be found in Refs. [21–31]. Here, we just present the salient features of the model. The model Hamiltonian is

$$H = \sum_{i=1}^{6}\left(m_i + \frac{p_i^2}{2m_i}\right) - T_c + \sum_{i<j} V_{ij}, \tag{1}$$

$$V_{ij} = V^G(r_{ij}) + V^\chi(r_{ij}) + V^C(r_{ij}),$$

$$V^G(r_{ij}) = \frac{1}{4}\alpha_s \boldsymbol{\lambda}_i\cdot\boldsymbol{\lambda}_j\left[\frac{1}{r_{ij}} - \frac{\pi}{2}\left(\frac{1}{m_i^2}+\frac{1}{m_j^2}+\frac{4\boldsymbol{\sigma}_i\cdot\boldsymbol{\sigma}_j}{3m_im_j}\right)\times\delta(r_{ij}) - \frac{3}{4m_im_jr_{ij}^3}S_{ij}\right],$$

$$V^\chi(r_{ij}) = \frac{\alpha_{ch}}{3}\frac{\Lambda^2}{\Lambda^2-m_\chi^2}m_\chi\left\{\left[Y(m_\chi r_{ij}) - \frac{\Lambda^3}{m_\chi^3}Y(\Lambda r_{ij})\right]\times\boldsymbol{\sigma}_i\cdot\boldsymbol{\sigma}_j + \left[H(m_\chi r_{ij}) - \frac{\Lambda^3}{m_\chi^3}H(\Lambda r_{ij})\right]S_{ij}\right\}\times\mathbf{F}_i\cdot\mathbf{F}_j, \quad \chi = \pi, K, \eta$$

$$V^C(r_{ij}) = -a_c\lambda_i\cdot\lambda_j[f(r_{ij}) + V_0],$$

$$f(r_{ij}) = \begin{cases} r_{ij}^2 & \text{if } i,j \text{ occur in the same baryon orbit} \\ \frac{1-e^{-\mu_{ij}r_{ij}^2}}{\mu_{ij}} & \text{if } i,j \text{ occur in different baryon orbits} \end{cases}$$

$$S_{ij} = \frac{(\sigma_i\cdot\mathbf{r}_{ij})(\sigma_j\cdot\mathbf{r}_{ij})}{r_{ij}^2} - \frac{1}{3}\sigma_i\cdot\sigma_j.$$

where S_{ij} is quark tensor operator; $Y(x)$ and $H(x)$ are standard Yukawa functions ([32] and reference there in); T_c is the kinetic energy of the center of mass; α_{ch} is the chiral coupling constant; determined as usual from the π–nucleon coupling constant; α_s is the quark–gluon coupling constant. In order to cover the wide energy range from light to heavy quarks one introduces an effective scale-dependent quark–gluon coupling $\alpha_s(\mu)$[33]:

$$\alpha_s(\mu) = \frac{\alpha_0}{\ln(\frac{\mu^2+\mu_0^2}{\Lambda_0^2})}, \tag{2}$$

where μ is the reduced mass of two interacting quarks. All other symbols have their usual meanings. Here, a phenomenological color screening confinement potential is used,

Table 1 Model parameters: $m_\pi = 0.7\ \text{fm}^{-1}$, $m_k = 2.51\ \text{fm}^{-1}$, $m_\eta = 2.77\ \text{fm}^{-1}$, $\Lambda_\pi = 4.2\ \text{fm}^{-1}$, $\Lambda_k = 5.2\ \text{fm}^{-1}$, $\Lambda_\eta = 5.2\ \text{fm}^{-1}$, $\alpha_{ch} = 0.027$

b (fm)	m_s (MeV)	m_c (MeV)	m_b (MeV)	a_c (MeV fm^{-2})
0.518	573	1700	5140	58.03
V_0 (MeV)	α_0	Λ_0 (fm^{-1})	u_0 (MeV)	
−1.2883	0.5101	1.525	445.808	

Table 2 The calculated masses (in MeV) of the charm and bottom baryons and mesons in QDCSM. Experimental values are taken from the Particle Data Group (PDG) [34]

	Σ_c	Σ_c^*	Λ_c	Ξ_c^*	Ξ_c	Ξ_c'
Exp.	2455	2520	2286	2645	2467	2575
Model	2378	2404	2200	2552	2464	2533
	Ω_c	Ω_c^*	D	D^*	D_s	D_s^*
Exp.	2695	2770	1864	2007	1968	2112
Model	2698	2709	1890	1924	2105	2119
	B	B^*	η_c	J/ψ	η_b	$\Upsilon(1s)$
Exp.	2980	3096	9391	9460	5279	5325
Model	3224	3227	10104	10104	5333	5344
	Σ_b	Σ_b^*	Λ_b	Ξ_b	Ω_b	
Exp.	5811	5832	5619	5791	6071	
Model	5808	5816	5618	5887	6130	

and μ_{ij} is the color screening parameter. For the light-flavor quark system, it is determined by fitting the deuteron properties, NN scattering phase shifts, $N\Lambda$ and $N\Sigma$ scattering phase shifts, respectively, with $\mu_{uu} = 0.45$, $\mu_{us} = 0.19$ and $\mu_{ss} = 0.08$, satisfying the relation, $\mu_{us}^2 = \mu_{uu} * \mu_{ss}$. When extending to the heavy quark case, there is no experimental data available, so we take it as a adjustable parameter. In the present work, we take $\mu_{cc} = 0.01 \sim 0.0001\ \text{fm}^{-2}$ and μ_{uc} is obtained by the relation $\mu_{uc}^2 = \mu_{uu} * \mu_{cc}$. All other parameters are also taken from our previous work [31], except for the charm and bottom quark masses m_c and m_b, which are fixed by a fitting to the masses of the charmed and bottom baryons and mesons. The values of those parameters are listed in Table 1. The calculated masses of the charmed and bottom baryons and mesons are shown in Table 2.

The quark delocalization in QDCSM is realized by specifying the single particle orbital wave function of QDCSM as a linear combination of left and right Gaussians, the single particle orbital wave functions used in the ordinary quark cluster model,

$$\begin{aligned}
\psi_\alpha(\mathbf{s}_i,\epsilon) &= \left(\phi_\alpha(\mathbf{s}_i) + \epsilon\phi_\alpha(-\mathbf{s}_i)\right)/N(\epsilon),\\
\psi_\beta(-\mathbf{s}_i,\epsilon) &= \left(\phi_\beta(-\mathbf{s}_i) + \epsilon\phi_\beta(\mathbf{s}_i)\right)/N(\epsilon),\\
N(\epsilon) &= \sqrt{1+\epsilon^2+2\epsilon e^{-s_i^2/4b^2}}.\\
\phi_\alpha(\mathbf{s}_i) &= \left(\frac{1}{\pi b^2}\right)^{3/4} e^{-\frac{1}{2b^2}(\mathbf{r}_\alpha-\mathbf{s}_i/2)^2}\\
\phi_\beta(-\mathbf{s}_i) &= \left(\frac{1}{\pi b^2}\right)^{3/4} e^{-\frac{1}{2b^2}(\mathbf{r}_\beta+\mathbf{s}_i/2)^2}.
\end{aligned} \tag{3}$$

Here $\mathbf{s}_i$, $i = 1, 2, \ldots, n$ are the generating coordinates, which are introduced to expand the relative motion wavefunction [23]. The mixing parameter $\epsilon(\mathbf{s}_i)$ is not an adjusted one but determined variationally by the dynamics of the multi-quark system itself. This assumption allows the multi-quark system to choose its favorable configuration in the interacting process. It has been used to explain the cross-over transition between hadron phase and quark–gluon plasma phase [35].

3 The results and discussions

Here, we investigate the possible hidden-charm molecular pentaquarks with $Y = 1$, $I = \frac{1}{2}$, $J^P = \frac{1}{2}^\pm$, $\frac{3}{2}^\pm$, and $\frac{5}{2}^\pm$. For the negative parity states, we calculate the S-wave channels with spin $S = \frac{1}{2}$, $\frac{3}{2}$, and $\frac{5}{2}$, respectively; and for the positive parity states, we calculate the P-wave channels with spin $S = \frac{1}{2}$, $\frac{3}{2}$, and $\frac{5}{2}$, respectively. All the channels involved are listed in Table 3. In the present calculation, we only consider the hidden-charm molecular pentaquarks which consist of two S-wave hadrons. The channel-coupling effects are also taken into account. However, we find there is not any bound state with the positive parity within our calculations. There may exist other molecular structures, which contain excited hadrons, such as $\chi_{c1}p$ resonance [16], $J/\psi N(1440)$, $J/\psi N(1520)$ [17] and so on, which are out of range of present calculation. In the following we only show the results of the negative parity states.

First, the effective potentials between two hadrons are calculated and shown in Figs. 1, 2 and 3, because an attractive potential is necessary for forming a bound state or resonance. The effective potential between two colorless clusters is defined by $V(s) = E(s) - E(\infty)$, where $E(s)$ is the energy of the system at the separation s of two clus-

Table 3 The channels involved in the calculation

$S = \frac{1}{2}$	$N\eta_c$	NJ/ψ	$\Lambda_c D$	$\Lambda_c D^*$	$\Sigma_c D$
	$\Sigma_c D^*$	$\Sigma_c^* D^*$			
$S = \frac{3}{2}$	NJ/ψ	$\Lambda_c D^*$	$\Sigma_c D^*$	$\Sigma_c^* D$	$\Sigma_c^* D^*$
$S = \frac{5}{2}$	$\Sigma_c^* D^*$				

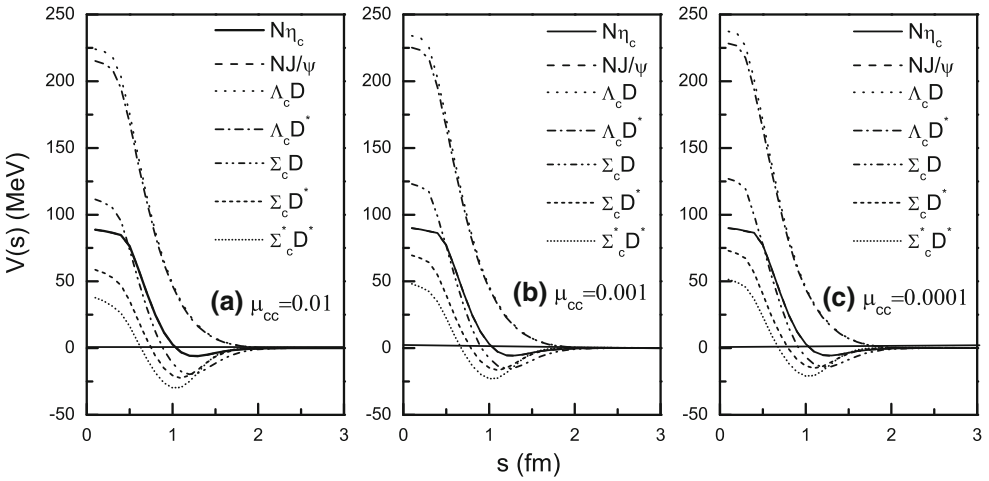

Fig. 1 The potentials of different channels for the $IJ^P = \frac{1}{2}\frac{1}{2}^-$ system

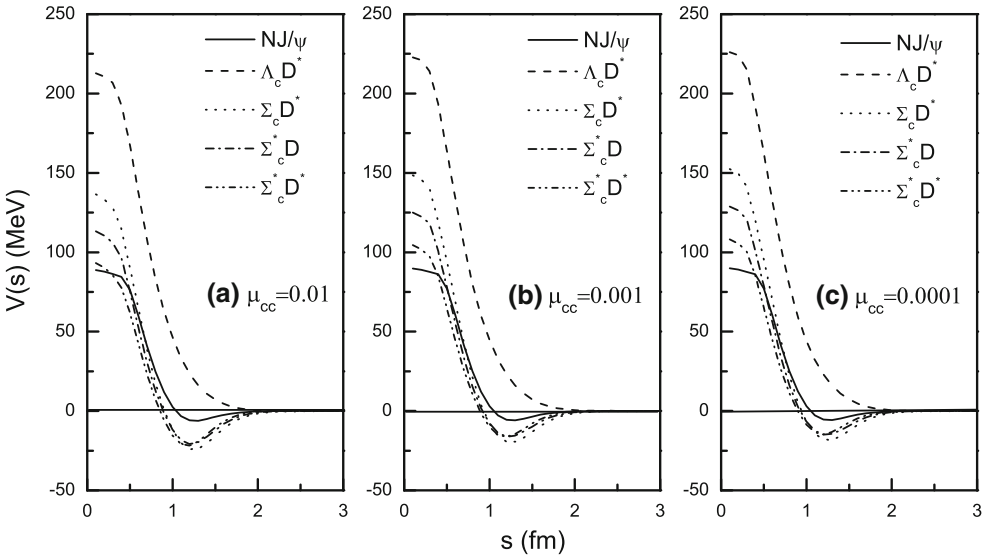

Fig. 2 The potentials of different channels for the $IJ^P = \frac{1}{2}\frac{3}{2}^-$ system

ters, which is obtained by the adiabatic approximation. As mentioned in Sect. 2, a phenomenological color screening confinement potential is introduced in our model. For the multi-quark systems with heavy quark, because no experimental data is available, so we take three different values of μ_{cc} ($\mu_{cc} = 0.01,\ 0.001,\ 0.0001$), to check the dependence of our results on this parameter.

For the $J^P = \frac{1}{2}^-$ system (Fig. 1), one sees that the potentials are all attractive for the channels $N\eta_c$, NJ/ψ, $\Sigma_c D$, $\Sigma_c D^*$ and $\Sigma_c^* D^*$. For the channels $\Lambda_c D$ and $\Lambda_c D^*$, the potentials are repulsive, so no bound states or resonances can be formed in these two channels. However, the bound states or resonances are possible for other channels due to the attractive nature of the interaction between two hadrons. The attraction between Σ_c^* and D^* is the largest one, followed by that of the $\Sigma_c D^*$ channel, which is a little larger than that of the $\Sigma_c D$ channel. In addition, the attraction of $N\eta_c$ is almost the same as that of NJ/ψ, which is the smallest one during these five attractive channels. Comparing figures (a), (b), and (c) in Fig. 1, we also find that larger values of μ_{cc} give rise lower energy, although the variation is not very significant.

For the $J^P = \frac{3}{2}^-$ system (Fig. 2), similar results to that of $IJ^P = \frac{1}{2}\frac{1}{2}^-$ system are obtained. The potentials are all attractive for channels NJ/ψ, $\Sigma_c D^*$, $\Sigma_c^* D$ and $\Sigma_c^* D^*$, while for the $\Lambda_c D^*$ channel, it is strongly repulsive. For the dependence of potentials on the different values of μ_{cc}, the behavior is the same as that of the $J^P = \frac{1}{2}^-$ system.

For the $J^P = \frac{5}{2}^-$ system (Fig. 3), there is only one channel $\Sigma_c^* D^*$, the potentials are attractive, and the dependences of the potentials on μ_{cc} are similar to that in $J^P = \frac{1}{2}^-$ and $J^P = \frac{3}{2}^-$ system.

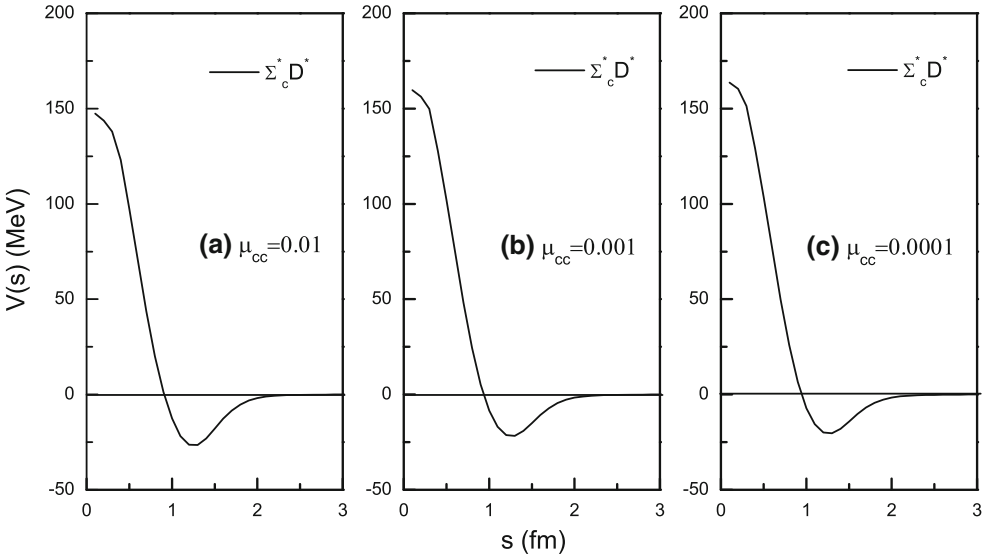

Fig. 3 The potential of a single channel for the $IJ^P = \frac{1}{2}\frac{5}{2}^-$ system

Table 4 The binding energies and the masses (in MeV) of the hidden-charm molecular pentaquarks of $I = \frac{1}{2}$

$J^P = \frac{1}{2}^-$				$J^P = \frac{3}{2}^-$			
μ_{cc}	0.01	0.001	0.0001	μ_{cc}	0.01	0.001	0.0001
$N\eta_c$	ub	ub	ub	NJ/ψ	ub	ub	ub
NJ/ψ	ub	ub	ub	$\Lambda_c D^*$	ub	ub	ub
$\Lambda_c D$	ub	ub	ub	$\Sigma_c D^*$	−16/4303	−11/4308	−10/4309
$\Lambda_c D^*$	ub	ub	ub	$\Sigma_c^* D$	−17/4445	−14/4448	−12/4450
$\Sigma_c D$	−19/4300	−15/4304	−13/4306	$\Sigma_c^* D^*$	−17/4510	−15/4512	−13/4514
$\Sigma_c D^*$	−21/4441	−19/4443	−18/4444	$J^P = \frac{5}{2}^-$			
$\Sigma_c^* D^*$	−24/4503	−23/4504	−21/4506	$\Sigma_c^* D^*$	−15/4512	−10/4517	−10/4517

In order to see whether or not there are any bound states or resonances, a dynamic calculation is needed. The resonating group method (RGM), described in more detail in Ref. [36], is used here. Expanding the relative motion wavefunction between two clusters in the RGM by gaussians, the integro-differential equation of the RGM can be reduced to an algebraic equation, the generalized eigen-equation. The energy of the system can be obtained by solving the eigen-equation. In the calculation, the baryon–meson separation ($|\mathbf{s}_n|$) is taken to be less than 6 fm (to keep the matrix dimension sufficiently small, so that we can still manage this case).

For the $J^P = \frac{1}{2}^-$ system, the single-channel calculation shows that both $\Lambda_c D$ and $\Lambda_c D^*$ are unbound, which agree with the repulsive nature of the interaction of these two channels. For the $N\eta_c$ and the NJ/ψ channels, the attractions are too weak to tie the two particles together, the calculation shows that they are also unbound. While, due to the stronger attractions, the obtained lowest energies of $\Sigma_c D$, $\Sigma_c D^*$ and $\Sigma_c^* D^*$ are below their corresponding thresholds. The binding energies of these three states are listed in Table 4, in which '*ub*' means unbound. Here we should mention how we obtain the mass of a hidden-charm molecular pentaquark. Generally, the mass of a molecular pentaquark can be written as $M^{\text{the.}} = M_1^{\text{the.}} + M_2^{\text{the.}} + B$, where $M_1^{\text{the.}}$ and $M_2^{\text{the.}}$ stand for the theoretical masses of a charmed baryon and an anti-charmed meson, respectively, and B is the binding energy of this molecular state. In order to minimize the theoretical errors and to compare calculated results to the experimental data, we shift the mass of molecular pentaquark to $M = M_1^{\text{exp.}} + M_2^{\text{exp.}} + B$, where the experimental values of charmed baryons and anti-charmed mesons are used. Taking the state $J^P = \frac{1}{2}^-$ $\Sigma_c D$ as an example, the calculated mass of the pentaquark is 4249 MeV, then the binding energy B is obtained by subtracting the theoretical masses of Σ_c and D, $4249 - 2378 - 1890 = -19$ (MeV). Adding the experimental masses of the hadrons, the mass of the pentaquark $M = 2455 + 1864 + (-19) = 4300$ (MeV) is arrived at. In the present calculation, the resonance masses for $\Sigma_c D$, $\Sigma_c D^*$ and $\Sigma_c^* D^*$ with $J^P = \frac{1}{2}^-$ are 4300–4306, 4441–4444, and 4503–4506 MeV, respectively. These results

Table 5 The masses (in MeV) of the hidden-charm molecular pentaquarks of $J^P = \frac{1}{2}^-$ with three closed channels coupling and the percentages of each channel in the eigen-states

$\mathrm{l}\mu_{cc}$	0.01			0.001			0.0001		
M_{cc}	4296	4437	4500	4300	4439	4501	4302	4440	4503
$\Sigma_c D$	95.5	2.9	4.8	96.0	2.5	4.5	96.7	2.1	4.2
$\Sigma_c D^*$	3.6	95.1	0.8	3.2	95.3	1.0	2.7	95.7	1.1
$\Sigma_c^* D^*$	0.9	2.0	94.4	0.8	2.2	94.5	0.6	2.2	94.7

Table 6 The masses (in MeV) of the hidden-charm molecular pentaquarks with all channels coupling and the percentages of each channel in the eigen-states

$J^P = \frac{1}{2}^-$				$J^P = \frac{3}{2}^-$				$J^P = \frac{5}{2}^-$			
μ_{cc}	0.01	0.001	0.0001	μ_{cc}	0.01	0.001	0.0001	μ_{cc}	0.01	0.001	0.0001
M_{cc}	3881	3883	3884	M_{cc}	3997	3998	3998	M_{cc}	4512	4517	4517
$N\eta_c$	41.7	49.7	35.2	NJ/ψ	80.8	71.0	62.1	$\Sigma_c^* D^*$	100.0	100.0	100.0
NJ/ψ	23.1	24.4	29.3	$\Lambda_c D^*$	8.7	11.9	15.9				
$\Lambda_c D$	14.6	11.7	14.5	$\Sigma_c D^*$	1.2	1.9	2.6				
$\Lambda_c D^*$	0.9	0.4	2.0	$\Sigma_c^* D$	3.5	5.8	7.3				
$\Sigma_c D$	0.1	4.8	6.0	$\Sigma_c^* D^*$	5.8	9.4	12.1				
$\Sigma_c D^*$	4.5	6.4	12.4								
$\Sigma_c^* D^*$	15.1	2.6	0.6								

are qualitatively similar to the conclusion of Ref. [5,6], in which they predicted two new N^* states (the $\Sigma_c D$ molecular state $N^*(4265)$ and the $\Sigma_c D^*$ molecular state $N^*(4415)$) in the coupled-channel unitary approach. Meanwhile, the chiral quark-model calculation also supported the existence of the S-wave $\Sigma_c D$ bound state [37].

At the same time, we also do a channel-coupling calculation. In this work, two kinds of channel coupling are performed. The first one is the coupling of three closed channels ($\Sigma_c D$, $\Sigma_c D^*$ and $\Sigma_c^* D^*$). The results, the lowest three eigen-energies and the percentages of coupling channels for the three eigen-states, are shown in Table 5. Taking the results of $\mu_{cc} = 0.01$ as an example, we can see that the main component of the lowest eigen-states is $\Sigma_c D$, ~95.5%, and the energy is pushed down a little, compared with the single-channel calculation, 4300–4296. The main component of the second lowest state is $\Sigma_c D^*$ with the percentage of 95.1%; and the main component of the third lowest state is $\Sigma_c^* D^*$ with the percentage of 94.4%. The three eigen-energies are all smaller than the thresholds of the corresponding main channels, and they are stable against the change of the baryon–meson separations. The large percentage of the main component and the small change of energy lead us to infer that the channel coupling is very weak. However, these three closed channels can be coupled to the other four open channels, $N\eta_c$, NJ/ψ, $\Lambda_c D$ and $\Lambda_c D^*$. The results of this channel-coupling calculation are shown in Table 6. We obtain a stable state, the mass of which is lower than the threshold of $N\eta_c$, and the main component of this state is $N\eta_c$, with the percentage of 41.7%. This shows that $N\eta_c$ of $J^P = \frac{1}{2}^-$ is bounded by channel coupling in our quark-model calculation, the energy is 3881–3884 (MeV). In addition, we also obtain several quasi-stable states, the masses of which are smaller than the thresholds of the corresponding main channels, but they fluctuate around the eigen-energies obtained in the three closed channel-coupling calculation. For example, the energy of one quasi-stable state is 4296 MeV, it fluctuates around this energy with 2 MeV with the variation of the baryon–meson separation. To confirm whether the states of $\Sigma_c D$, $\Sigma_c D^*$ and $\Sigma_c^* D^*$ can survive as resonance states after the full channel coupling, the study of the scattering processes of the open channels of $N\eta_c$, NJ/ψ, $\Lambda_c D$ and $\Lambda_c D^*$ is needed. This work is under way. From the fluctuation, we can estimate the partial decay widths of these states to $N\eta_c$, NJ/ψ, $\Lambda_c D$ and $\Lambda_c D^*$ are around several MeVs, if they are resonances.

For the $J^P = \frac{3}{2}^-$ system, similar results to the case of $J^P = \frac{1}{2}^-$ system are obtained. The single-channel calculation shows that NJ/ψ and $\Lambda_c D^*$ are unbound, while $\Sigma_c D^*$, $\Sigma_c^* D$ and $\Sigma_c^* D^*$ are all bound. The results are also listed in Table 4. These three states also exist when they are coupled together, the masses and the percentages of each channel of the lowest three eigen-states are shown in Table 7. We can see that the mass of the first eigen-state is about 4362–4368 MeV and the main channel is $\Sigma_c^* D$ with the percentage of 91.0–95.5%; the mass of the second eigen-state is about 4445–4451 MeV and the main channel is $\Sigma_c D^*$ with the percentage of 96.2–98.5%; the mass of the third eigen-state is about 4551–4555 MeV and the main channel is $\Sigma_c^* D^*$ with the percentage of 94.6–96.2%. From the above results, we find that the mass of the first eigen-state is close to the mass of the observed $P_c(4380)$, a pentaquark reported by the LHCb Collaboration. Therefore, in our quark-model calculation the main component of the $P_c(4380)$ is $\Sigma_c^* D$ with the quantum number

Table 7 The masses (in MeV) of the hidden-charm molecular pentaquarks of $J^P = \frac{3}{2}^-$ with three closed channels coupling and the percentages of each channel in the eigen-states

μ_{cc}	0.01			0.001			0.0001		
M_{cc}	4362	4445	4551	4365	4450	4553	4368	4451	4554
$\Sigma_c D^*$	3.8	96.2	1.4	1.6	98.0	1.0	1.2	98.5	0.8
$\Sigma_c^* D$	91.0	2.8	4.0	94.1	1.0	3.7	95.5	0.7	3.0
$\Sigma_c^* D^*$	5.2	1.0	94.6	4.3	1.0	95.3	3.3	0.8	96.2

$J^P = \frac{3}{2}^-$. In addition, the mass of the second eigen-state is close to the mass of another reported pentaquark $P_c(4450)$. Nevertheless, the opposite parity of the state to $P_c(4380)$ may prevent one from making this assignment. Moreover, all these closed channels can be coupled to the open channels NJ/ψ and $\Lambda_c D^*$. The results of the couplings of these five channels are shown in Table 6. There is a stable state, the mass of which is lower than the threshold of NJ/ψ, and the main channel of this state is NJ/ψ, with the ratio of 80.8–62.1%. This shows that the NJ/ψ of $J^P = \frac{3}{2}^-$ is bounded by channel coupling. However, it can couple to the D-wave $N\eta_c$. So further work should be done to check whether the $J^P = \frac{3}{2}^-$ NJ/ψ is a resonance state in the D-wave $N\eta_c$ scattering process. In fact, the possible existence of a nuclear bound quarkonium state was proposed more than 20 years ago by Brodsky et al. [38]; Gao et al. [39] also predicted the existence of the $N\phi$ bound state, which is very similar to the NJ/ψ state; and the recent lattice QCD calculation also supported the existence of the strangenium–nucleus and the charmonium–nucleus bound states [40]. Therefore, searching for the NJ/ψ resonance state is interesting work for the future. In addition, there are also several quasi-stable states in the full channel-coupling calculation, the masses of which are lower than the thresholds of the corresponding main channels and they fluctuate several MeVs around their central values. It is just the behavior of a resonance. The amplitude of the fluctuation can be taken as the decay width of the quasi-states. In a quark-model calculation, the decay width of the $P_c(4380)$ candidate is too small to match the experimental value. Further study is needed to check whether these eigen-states are resonance states in the NJ/ψ and $\Lambda_c D^*$ scattering process and to calculate the widths of other decay modes.

As mentioned above, by taking into account the channel-coupling effect, a bound state $N\eta_c$ is obtained for the $J^P = \frac{1}{2}^-$ system; and another bound state NJ/ψ is obtained for the $J^P = \frac{3}{2}^-$ system. In these two systems, the coupling between the calculated S-wave channels is through the central force. In order to see the strength of this channel coupling, we calculate the transition potentials of these channels. Here, we take the result of the $J^P = \frac{3}{2}^-$ system with $\mu_{cc} = 0.01$ as an example. The transition potentials of five channels NJ/ψ, $\Lambda_c D^*$, $\Sigma_c D^*$, $\Sigma_c^* D$, and $\Sigma_c^* D^*$ are shown in Fig. 4. Obviously, it is a strong coupling among these channels that makes

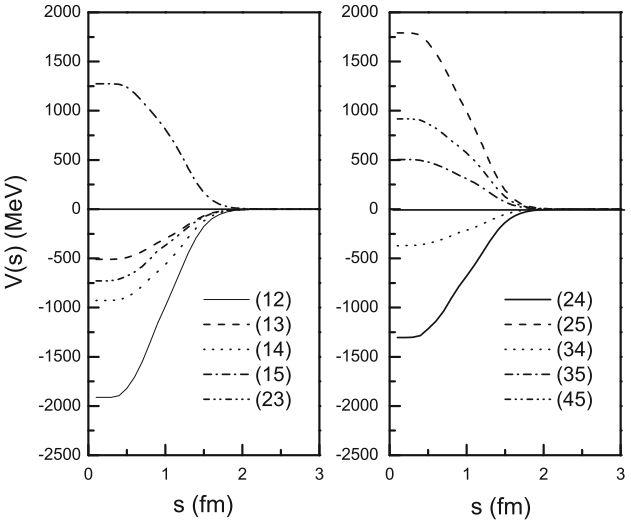

Fig. 4 The transition potentials of channels NJ/ψ, $\Lambda_c D^*$, $\Sigma_c D^*$, $\Sigma_c^* D$, and $\Sigma_c^* D^*$, which are labeled channels 1, 2, 3, 4, and 5 respectively

NJ/ψ the bound state. The mechanism to form a bound state has been proposed before. Swanson proposed that the admixtures of $\rho J/\psi$ and $\omega J/\psi$ states were important for forming $X(3872)$ state [41], which was also demonstrated in Ref. [42] by Fernández-Caramés et al. The mechanism also applied to the study of H-dibaryon [43], in which the single channel $\Lambda\Lambda$ is unbound, but when coupled to the channels $N\Xi$ and $\Sigma\Sigma$, it becomes a bound state. The effect of channel coupling of the $J^P = \frac{3}{2}^-$ system is the same as the one of the $J^P = \frac{1}{2}^-$ system.

For the $J^P = \frac{5}{2}^-$ system, it includes only one channel $\Sigma_c^* D^*$, and it is a bound state with the mass of 4512–4517 (MeV), which is a little higher than that of $P_c(4450)$. Although the width of the S-wave $\Sigma_c^* D^*$ decaying to the D-wave $N\eta_c$ and $J/\psi p$ (tensor interaction induced decay) is generally small, which can be used to explain why the width of $P_c(4450)$ is much narrower than that of $P_c(4380)$, $J^P = \frac{5}{2}^-$ may not be a good candidate of $P_c(4450)$ because of the opposite parity of the state to $P_c(4380)$.

In the previous discussion, the hidden-charm molecular pentaquarks were investigated. We also extend the study to the hidden-bottom pentaquarks because of the heavy flavor symmetry. Here we take the value of $\mu_{bb} = 0.0001$. The numerical results are listed in Tables 8, 9, and 10. The results are similar to the hidden-charm molecular pentaquarks. For

Table 8 The binding energies (in MeV) of the hidden-bottom molecular pentaquarks of $I = \frac{1}{2}$

$J^P = \frac{1}{2}^-$		$J^P = \frac{3}{2}^-$		$J^P = \frac{5}{2}^-$	
$N\eta_b$	ub	$N\Upsilon(1s)$	ub	$\Sigma_b^* B^*$	−14
$N\Upsilon(1s)$	ub	$\Lambda_b B^*$	ub		
$\Lambda_b B$	ub	$\Sigma_b B^*$	−14		
$\Lambda_b B^*$	ub	$\Sigma_b^* B$	−15		
$\Sigma_b B$	−15	$\Sigma_b^* B^*$	−16		
$\Sigma_b B^*$	−21				
$\Sigma_b^* B^*$	−24				

Table 9 The masses (in MeV) of the hidden-bottom molecular pentaquarks with three closed channels coupling and the percentages of each channel in the eigen-states

M_{cc}	11,070	11,112	11,132
$J^P = \frac{1}{2}^-$			
$\Sigma_b B$	76.8	12.4	8.1
$\Sigma_b B^*$	21.7	67.7	10.2
$\Sigma_b^* B^*$	1.5	19.9	81.7
M_{cc}	11,091	11,121	11,138
$J^P = \frac{3}{2}^-$			
$\Sigma_b B^*$	5.1	86.5	9.5
$\Sigma_b^* B$	78.4	7.8	8.7
$\Sigma_b^* B^*$	16.5	5.7	81.8

Table 10 The masses (in MeV) of the hidden-bottom molecular pentaquarks of $I = \frac{1}{2}$ and the percentages of each channel in the eigen-states

$J^P = \frac{1}{2}^-$		$J^P = \frac{3}{2}^-$		$J^P = \frac{5}{2}^-$	
M_{cc}	10,304	M_{cc}	10,382	M_{cc}	11,143
$N\eta_b$	33.8	$N\Upsilon(1s)$	34.6	$\Sigma_b^* B^*$	100.0
$N\Upsilon(1s)$	14.7	$\Lambda_b B^*$	32.6		
$\Lambda_b B$	24.2	$\Sigma_b B^*$	18.7		
$\Lambda_b B^*$	5.2	$\Sigma_b^* B$	13.7		
$\Sigma_b B$	2.1	$\Sigma_b^* B^*$	0.4		
$\Sigma_b B^*$	0.7				
$\Sigma_b^* B^*$	19.3				

the $J^P = \frac{1}{2}^-$ system, a bound state is obtained by all channels coupling, and the main channel is $N\eta_b$ with the mass of 10,304 MeV; the quasi-stable states with main components of $\Sigma_b B$, $\Sigma_b B^*$ and $\Sigma_b^* B^*$, respectively should be confirmed by calculating the open channels scattering in future. For the $J^P = \frac{3}{2}^-$ system, there is also a bound state of 10,382 MeV, and the main channel is $N\Upsilon(1s)$, which also should be checked whether it is a resonance state or not in the D-wave $N\eta_b$ scattering process. Moreover, further work should be done to check whether the quasi-stable states of $\Sigma_b B^*$, $\Sigma_b^* B$, and $\Sigma_b^* B^*$ are resonance states or not in the $N\Upsilon(1s)$ and $\Lambda_b B^*$ scattering process. For the $J^P = \frac{5}{2}^-$ system, a bound state $\Sigma_b^* B^*$ is obtained, with the mass of 11,143 MeV.

4 Summary

In summary, the possible hidden-charm molecular pentaquarks with $Y = 1$, $I = \frac{1}{2}$, $J^P = \frac{1}{2}^\pm$, $\frac{3}{2}^\pm$, and $\frac{5}{2}^\pm$ are investigated by solving the RGM equation in the framework of QDCSM. Our results show: (1) All the positive parity states are all unbound in our calculation. Some other molecular structures, which contain excited hadrons, such as $\chi_{c1} p$, $J/\psi N(1440)$, $J/\psi N(1520)$ and so on, would deserve further study. (2) For the $J^P = \frac{1}{2}^-$ system, there is a bound state of 3881–3884 MeV by seven channels coupling, and the main channel is $N\eta_c$; there are three quasi-stable states of $\Sigma_c D$, $\Sigma_c D^*$ and $\Sigma_c^* D^*$ should be confirmed by investigating the scattering process of the open channels of $N\eta_c$, NJ/ψ, $\Lambda_c D$ and $\Lambda_c D^*$. (3) For the $J^P = \frac{3}{2}^-$ system, the main channel of the bound state is NJ/ψ with the mass of 3997–3998 MeV, which may be a resonance state in the D-wave $N\eta_c$ scattering process. There are also three quasi-stable states: $\Sigma_c D^*$ with the mass of 4362–4368 MeV, $\Sigma_c^* D$ with the mass of 4445–4451 MeV, and $\Sigma_c^* D^*$ with the mass of 4551–4555 MeV, of which the mass of $\Sigma_c D^*$ is close to the observed $P_c(4380)$. So in our quark-model calculation $P_c(4380)$ can be explained as the molecular pentaquark $\Sigma_c^* D$ with the quantum number $J^P = \frac{3}{2}^-$. However, the partial decay width of $\Sigma_c D^*$ to NJ/ψ is estimated to be several MeVs, which should be checked by further experiments. Similarly, the open channels of the NJ/ψ and $\Lambda_c D^*$ scattering process calculation is needed to confirm the resonance states of $\Sigma_c D^*$, $\Sigma_c^* D$, and $\Sigma_c^* D^*$. (4) For the $J^P = \frac{5}{2}^-$ system, there is a bound state $\Sigma_c^* D^*$ with the mass of 4512–4517 (MeV). However, it may not a good candidate of the observed $P_c(4450)$ because of the opposite parity of the state to $P_c(4380)$. Besides, the calculation is also extended to the hidden-bottom pentaquarks. The results are similar to the case of the hidden-charm molecular pentaquarks.

QDCSM, which was developed to study the multi-quark states, is an extension of the naïve quark model. As is well known, the quark model plays an important role in the development of hadron physics. The discovery of Ω^- is based on the prediction of the quark concept of Gell–Mann–Zweig. The naïve quark model of Isgur et al. gave a remarkable description of the properties of ground-state hadrons. On application to the excited states of hadron, hadron–hadron interaction, and multi-quark systems, extensions to the naïve quark model have to be made. Based on the different extension of the naive quark model, a proliferation of bound states

or resonances are predicted. The recent progress of experiments on "XYZ" particles, P_c^+ pentaquarks, and dibaryons such as $d*$ [44–46] is encouraging. However, some precaution as regards the proliferation of quark-model bound states has to be posed. So far, there is no multi-quark state unambiguously identified by the experiments. For particular multi-quark state, there exist different points of view. For example, Vijande et al. studied the four-quark system $c\bar{c}n\bar{n}$ in the constituent quark model by using different types of quark–quark potentials, and no four-quark bound states have been found [47], whereas the diquark–antidiquark picture was used by Maiani et al. to explain the state $X(3872)$ [48]. Vijande et al. also searched for the doubly heavy dibaryons in a simple quark model, but no bound or metastable state was found [49], whereas H-like dibaryons with heavy quarks were proposed in Ref. [50]. More theoretical and experimental work are needed to distinguish the different extension of the quark model. The critical development of the quark model may be the unquenching quark model, where the valence quarks and real/virtual quark pair are treated equally. Caramés and Valcarce have studied the possible multi-quark contributions to the charm baryon spectrum by considering higher order Fork space components [51]. By incorporating new ingredients, the phenomenological quark model is expected to describe ordinary and exotic hadrons well.

Acknowledgements The work is supported partly by the National Natural Science Foundation of China under Grant Nos. 11175088, 11535005, and 11205091, the Natural Science Foundation of the Jiangsu Higher Education Institutions of China (Grant No. 16KJB140006), and Jiangsu Government Scholarship for Overseas Studies.

References

1. D. Qing, X.S. Chen, F. Wang, Phys. Rev. C **57**, R31 (1998)
2. D. Qing, X.S. Chen, F. Wang, Phys. Rev. D **58**, 114032 (1998)
3. B.S. Zou, D.O. Riska, Phys. Rev. Lett. **95**, 072001 (2005)
4. T. Nakano et al. (LEPS Collaboration), Phys. Rev. C. **79**, 025210 (2009)
5. J.J. Wu, R. Molina, E. Oset, B.S. Zou, Phys. Rev. Lett. **105**, 232001 (2010)
6. J.J. Wu, R. Molina, E. Oset, B.S. Zou, Phys. Rev. C **84**, 015202 (2011)
7. Z.C. Yang, Z.F. Sun, J. He, X. Liu, S.L. Zhu, Chin. Phys. C **36**, 6 (2012)
8. T. Uchino, W.H. Liang, E. Oset, Eur. Phys. J. A **52**, 43 (2016)
9. M. Karliner, J.L. Rosner, Phys. Rev. Lett. **115**, 122001 (2015)
10. R. Aaij et al. (LHCb Collaboration), Phys. Rev. Lett. **115**, 072001 (2015)
11. H.X. Chen, W. Chen, X. Liu, S.L. Zhu, Phys. Rep. **639**, 1 (2016)
12. R. Chen, X. Liu, X.Q. Li, S.L. Zhu, Phys. Rev. Lett. **115**, 132001 (2015)
13. J. He, Phys. Lett. B. **753**, 547 (2016)
14. H.X. Chen, W. Chen, X. Liu, T.G. Steel, S.L. Zhu, Phys. Rev. Lett. **115**, 172001 (2015)
15. L. Roca, J. Nieves, E. Oset, Phys. Rev. D **92**, 094003 (2015)
16. U.-G. Meißner, J.A. Oller, Phys. Lett. B **751**, 59 (2015)
17. V. Kubarovsky, M.B. Voloshin, Phys. Rev. D **92**, 031502 (2015)
18. F.K. Guo, U.-G. Meißner, W. Wang, Z. Yang, Phys. Rev. D **92**, 071502 (2015)
19. X.H. Liu, Q. Wang, Q. Zhao, Phys. Lett. B **757**, 231 (2016)
20. T.J. Burns, Eur. Phys. J. A **51**, 152 (2015)
21. F. Wang, G.H. Wu, L.J. Teng, T. Goldman, Phys. Rev. Lett. **69**, 2901 (1992)
22. G.H. Wu, L.J. Teng, J.L. Ping, F. Wang, T. Goldman, Phys. Rev. C **53**, 1161 (1996)
23. H.X. Huang, P. Xu, J.L. Ping, F. Wang, Phys. Rev. C **84**, 064001 (2011)
24. J.L. Ping, F. Wang, T. Goldman, Nucl. Phys. A **657**, 95 (1999)
25. G.H. Wu, J.L. Ping, L.J. Teng et al., Nucl. Phys. A **673**, 279 (2000)
26. H.R. Pang, J.L. Ping, F. Wang, T. Goldman, Phys. Rev. C **65**, 014003 (2001)
27. J.L. Ping, F. Wang, T. Goldman, Nucl. Phys. A **688**, 871 (2001)
28. J.L. Ping, H.R. Pang, F. Wang, T. Goldman, Phys. Rev. C **65**, 044003 (2002)
29. L.Z. Chen, H.R. Pang, H.X. Huang, J.L. Ping, F. Wang, Phys. Rev. C **76**, 014001 (2007)
30. J.L. Ping, H.X. Huang, H.R. Pang, F. Wang, C.W. Wong, Phys. Rev. C **79**, 024001 (2009)
31. M. Chen, H.X. Huang, J.L. Ping, F. Wang, Phys. Rev. C **83**, 015202 (2011)
32. A. Valcarce, H. Garcilazo, F. Fernández, P. Gonzalez, Rep. Prog. Phys. **68**, 965 (2005)
33. J. Vijande, F. Fernandez, A. Valcarce, J. Phys. G **31**, 481 (2005)
34. J. Beringer et al. Particle Data Group, Phys. Rev. D **86**, 010001 (2012)
35. M.M. Xu, M. Yu, L.S. Liu, Phys. Rev. Lett. **100**, 092301 (2008)
36. M. Kamimura, Supp. Prog. Theor. Phys. **62**, 236 (1977)
37. W.L. Wang, F. Hang, Z.Y. Zhang, B.S. Zou, Phys. Rev. C **84**, 015203 (2011)
38. S.J. Brodsky, I. Schmidt, G.F. de Teramond, Phys. Rev. Lett. **64**, 1011 (1990)
39. H. Gao, T.-S.H. Lee, V. Marinov, Phys. Rev. C **63**, 022201(R) (2001)
40. S.R. Beane, E. Chang, S.D. Cohen, W. Detmold, H.-W. Lin, K. Orginos, A. Parreno, M.J. Savage, Phys. Rev. D **91**, 114503 (2015)
41. E.S. Swanson, Phys. Lett. B **588**, 189 (2004)
42. T. Fernández-Caramés, A. Valcarce, J. Vijande, Phys. Rev. Lett. 103, 222001 (2009)
43. H.R. Pang, J.L. Ping, F. Wang, T. Goldman, E.G. Zhao, Phys. Rev. C **69**, 065207 (2004)
44. M. Bashkanov et al. (CELSIUS-WASA Collaboration), Phys. Rev. Lett. **102**, 052301 (2009)
45. P. Adlarson et al. (WASA-at-COSY Collaboration), Phys. Rev. Lett. **106**, 242302 (2011)
46. P. Adlarson et al. (WASA-at-COSY Collaboration), Phys. Rev. Lett. **112**, 202301 (2014)
47. J. Vijande, E. Weissman, N. Barnea, A. Valcarce, Phys. Rev. D **76**, 094022 (2007)
48. L. Maiani, F. Piccinini, A.D. Polosa, V. Riquer, Phys. Rev. D **71**, 014028 (2005)
49. J. Vijande, A. Valcarce, J.-M. Richard, P. Sorba, Phys. Rev. D **94**, 034038 (2016)
50. H.X. Huang, J.L. Ping, F. Wang, Phys. Rev. C **92**, 035201 (2014)
51. T.F. Caramés, A. Valcarce, Phys. Rev. D **90**, 014042 (2014)